Mechanical vs. Electronic Strain: Calculated Configurations of Alkynyl-Pt(II)-Phosphine Macrocycles

Eric A. Buchanan[a] and Josef Michl[a,b]*
[a] *Department of Chemistry, University of Colorado, Boulder, CO 80309-0215, United States*
[b] *Institute of Organic Chemistry and Biochemistry, Czech Academy of Sciences, Flemingovo nám. 2, 16610 Prague 6, Czech Republic*

Corresponding Author: josef.michl@colorado.edu

Abstract. Optimized geometries of macrocycles composed of four $Pt(PR_3)_2$ linkers and four rods terminated with ethynyl or pyridyl moieties have been calculated at the PBE0/Def2-TZVPP//PBE0/Def2-SVP level of density functional theory for all combinations of cis and trans configurations at the Pt centers. For uncharged complexes with four *p,p'*-bis(ethynyl)biphenyl rods and neutral Pt centers, the energy of the planar oval-shaped all-trans isomer lies 17 kcal/mol below that of the puckered square-shaped all-cis isomer. In this case, the electronic strain associated with the cis arrangement at the Pt atoms overrules the mechanical strain associated with the bending of triple bonds. For cationic complexes containing two bipyridyl and two *p,p'*-bis(ethynyl)biphenyl rods, with a +1 charge on each Pt center, a puckered rectangular structure with all-cis Pt centers is found to be 38 kcal/mol lower in energy than the isomer with all four Pt centers trans. The results have been analyzed in terms of three additive factors, referred to as electronic, mechanical, and electrostatic strain.

Introduction

Self-assembly of molecular rods and transition-metal connectors is known to be capable of producing large symmetrical polygonal molecules.[1,2,3,4,5,6,7,8] These complexes have many possible applications such as molecular encapsulation,[9] catalysis,[10] and construction of metal-organic frameworks (MOFs).[11,12] When first produced,[13] products assembled from four square planar $Pt(II)(PEt_3)_2$ linkers and four *p,p'*-bis(ethynyl)biphenyl rods, or two *p,p'*-bis(ethynyl)biphenyl rods and two bis(4-pyridyl)ethyne rods, were automatically assumed to be rectangular macrocycles with a cis configuration on all four Pt atoms, **1** and **2**, respectively, since the trans configuration on platinum seemed to strain the ring unreasonably and appeared unlikely to self-assemble. Similar products were obtained with bis(4-pyridyl)butadiyne rods. With considerable encouragement from the presently reported calculations, the macrocycle containing four *p,p'*-bis(ethynyl)biphenyl rods has been more recently recognized by detailed analysis of NMR spectra to actually have a trans configuration at each Pt atom and to possess strongly bent triple bonds, which give it a surprising oval shape.[14] At the same time, the products containing two *p,p'*-bis(ethynyl)biphenyl rods and two bis(4-pyridyl)ethyne (or bis(4-pyridyl)butadiyne) rods were shown not to be macrocycles, but a mixture of linear oligomers.

Presently, we report the details of the calculations that triggered the re-evaluation of the self-assembled structures, and extend them to all possible geometrical isomers.

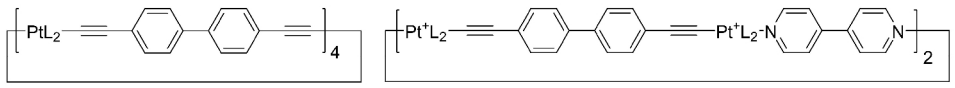

1 **2**

Figure 1. Chemical formulas for platinum macrocycles **1** and **2**. L represents phosphine ligands which can be oriented cis or trans.

Computational Details

All calculations used density functional theory (DFT) with the PBE0 hybrid functional[15] and were carried out using the quantum chemistry program ORCA.[16] This functional was selected because of its accuracy in calculating optimized geometries of transition-metal complexes.[17] It has also been found to perform well in calculating relative energies.[18] The Stuttgart effective core potential (ECP) Def2-SD[19] basis set was employed for platinum atoms along with the Ahlrichs-type valence basis sets Def2-SVP[20] and Def2-TZVPP.[21] Calculations on rods and ligands used the corresponding all-electron basis sets. Stuttgart-Dresden[22] type ECPs[23] perform well for transition-metal complex geometries when compared to all-electron results using ZORA (zeroth order regular approximation).[17,24] Geometry optimizations for the macrocycles were performed with the Def2-SVP basis set while all single point energy calculations were carried out using the Def2-TZVPP basis. These calculations all employed the RIJ-COSX[25,26] approximation to Coulomb and exchange integral evaluation along with the Def2/J[27] auxiliary basis. Geometry optimization and frequency analysis of all small molecules and fragments were performed with the Def2-TZVPP basis with no approximation to integral evaluation and a finer grid to ensure that they were true minima. The optimization of the macrocyclic geometries could not be converged when Grimme's DFT-D3BJ[28] dispersion correction was included in the calculations. Therefore, it was not included in any of the other calculations. The effect of the dispersion correction was nevertheless examined and determined to be inconsequential (see the Supporting Information). XYZ coordinates are provided in the Supporting Information.

Charge distributions were obtained from Mulliken[29] and Natural Bond Orbital (NBO)[30,31] population analysis using the density matrix produced by PBE0/Def2-TZVPP DFT calculations. Mulliken population analysis was performed by the ORCA program and NBO analysis was performed using the NBO 6.0 program[32] linked to ORCA.

For the neutral macrocycle **1**, there are 6 possible geometrical isomers that result from each of the four platinum metal centers being either cis or trans: $\mathbf{t_4}$, $\mathbf{ct_3}$, **ctct** (where two trans platinum atoms are opposite to each other), **cttc** (where two trans platinum atoms are adjacent to each other), $\mathbf{c_3t}$, and $\mathbf{c_4}$. In the cationic macrocycle **2**, there is one more, because the presence of two different rods allows two possible **cttc** isomers: one with a *p,p'*-bis(ethynyl)biphenyl rod between two adjacent trans platinum atoms, **ct:tc**, and another with a bis(4-pyridyl)ethyne rod between them, **ct·tc**. This would require geometry optimizations for 13 macrocycles with 276 and 268 atoms for **1** and **2**, respectively. The systems were reduced by 72 atoms each to a more manageable size by replacing the triethylphosphine with trimethylphosphine ligands. Optimized geometries for macrocycles with the two different phosphine ligands were compared for the all-trans and all-cis isomers of **1** and were found to be very similar, justifying this approximation.

Results

Isomer Geometries and Energies. Relative ground state energies for the twelve cis/trans isomers of neutral **1** and cationic **2** macrocycles found are shown in Table 1. All six possible isomers were found for **1** while only six of the possible seven were found for **2**. Of the two cationic isomers containing two cis and two trans Pt atoms with similar centers located on the same rod (**ct·tc** and **ct:tc**), we found the optimized geometry of only the isomer with the same platinum configurations on a bis(ethynyl)biphenyl rod, **ct:tc**. The geometry optimization of the **ct·tc** isomer, with similar centers connected by a bipyridyl rod, repeatedly failed to converge. This is likely due to excessive mechanical strain between the two trans centers associated with the extreme curvature required of the shorter bipyridyl rod. In the puckered rectangle-shaped $\mathbf{c_4}$ isomers of **1** and **2**, all six distances between two Pt atoms connected by a bis(ethynyl)biphenyl rod are 16.5 Å and the distance between two Pt atoms connected by a bipyridyl rod is only 11.3 Å. In the oval-shaped $\mathbf{t_4}$ isomers, the distances are 15.0, 15.0, 15.3, & 15.6 Å between Pt atoms connected by a bis(ethynyl)biphenyl rod and in $\mathbf{2t_4}$ they are 14.5 Å for Pt atoms connected by bis(ethynyl)biphenyl rods and 10.6 Å for those connected by bipyridyl rods.

The neutral macrocycle **1** is generally destabilized as the number of cis centers increases. However, the isomer containing two cis and two trans platinum centers in which similar centers are opposite to each other (**ctct**) deviates from this trend and is nearly the most stable isomer. The trend is reversed in the cationic macrocycle **2**, though again the energy of the **ctct** isomer is very close to that of the lowest energy isomer. Figure 2 shows the optimized structures of the twelve macrocycles. Front and side views are provided to show the three dimensional structure. Larger images are provided in the Supporting Information.

Table 1. Relative PBE0/Def2-TZVPP//PBE0/Def2-SVP Energies of Macrocycles (kcal/mol).[a]

1	E_{rel}	**2**	E_{rel}
$\mathbf{t_4}$	0.0	$\mathbf{t_4}$	37.6
$\mathbf{ct_3}$	4.2	$\mathbf{ct_3}$	24.5
ctct	0.4	**ctct**	0.4
cttc	9.8	**ct:tc**	13.8
$\mathbf{c_3t}$	11.4	$\mathbf{c_3t}$	3.0
$\mathbf{c_4}$	17.2	$\mathbf{c_4}$	0.0

[a] The energy of the most stable isomer is -6620.564 a.u. for **1** and -6381.777 a.u. for **2**.

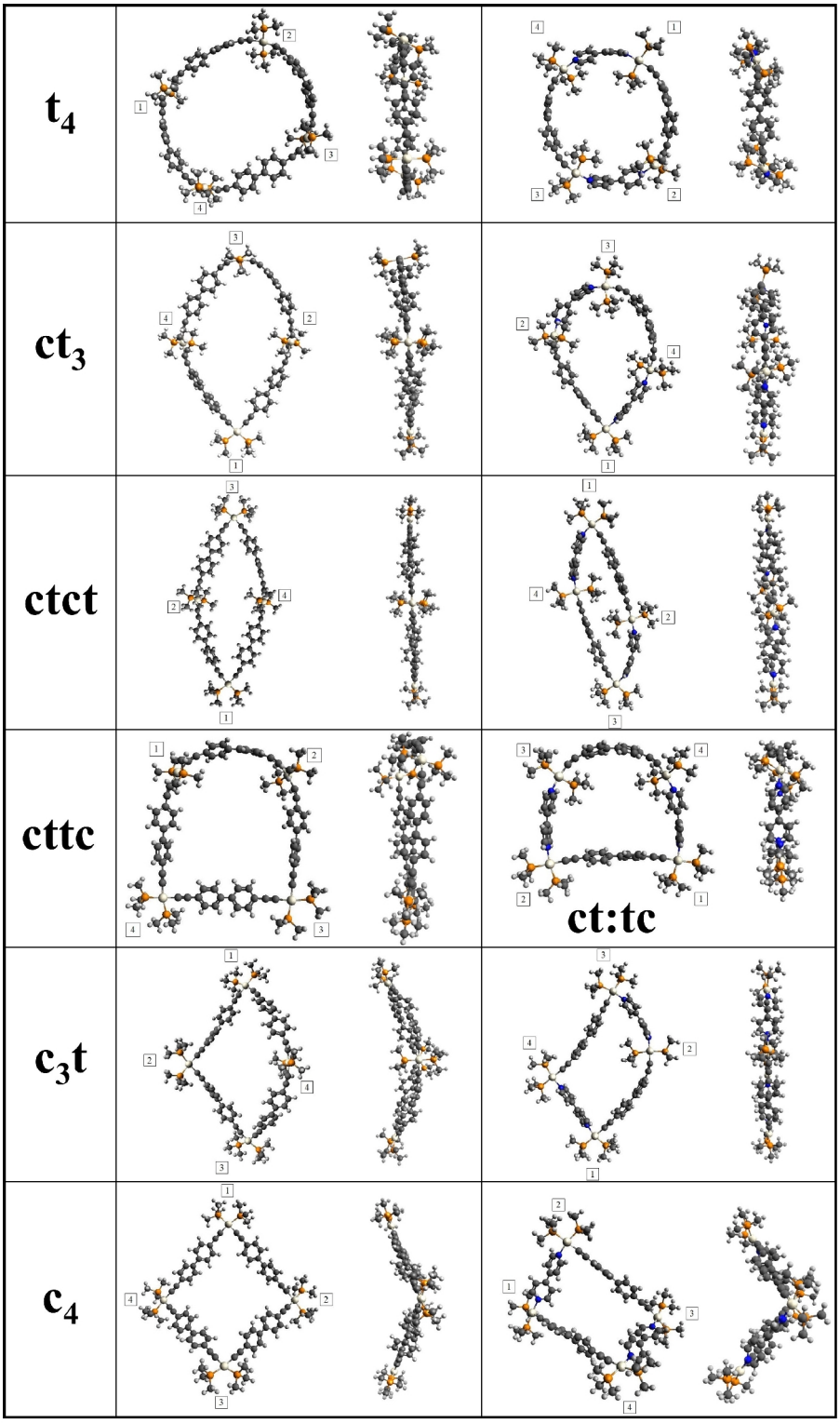

Figure 2. PBE0/Def2-SVP structures for isomers of **1** (left) and **2** (right). Platinum atom centers are labeled 1 to 4.

Eight of the twelve macrocycles are mostly planar. The exceptions are **1cttc**, **1c$_3$t**, **1c$_4$**, and **2c$_4$**. Interestingly, three of the four non-planar structures are isomers of the neutral macrocycle **1**, while only one is an isomer of the cationic macrocycle **2**. The **1cttc** macrocycle deviates slightly from planarity but its cationic counterpart, **2ct:tc**, is planar. Also, the neutral macrocycles **1c$_3$t** and **1c$_4$** are both puckered while only **2c$_4$** is puckered among the cationic species. Rods which are between two cis platinum centers are the least bent and strained. As the number of trans platinum atoms in a macrocycle increases, the ring strain must also increases as a result of the curvature required to close the cycle. Cis platinum atoms allow for less curved macrocycle geometries and therefore less ring strain; however, isomers with more cis platinum centers are only preferred over those with more trans platinum atoms in the cationic macrocycle **2**.

Electronic Strain. In order to elucidate the competition between electronic and mechanical strain in the macrocycles, platinum-based fragments of the macrocycles were also calculated (Figure 3). They consist of a platinum center with two trimethylphosphine ligands and one half of either two bis(ethynyl)biphenyl rods for the neutral species **1** or one half each of a bis(ethynyl)biphenyl and a bipyridyl rod for **2**. The half-rods are made by cutting the central C-C bond in the rod and capping with a terminal hydrogen. Table 2 gives the relative energies of the cis and trans isomers of the fragments with all coordinates optimized. These structures are assumed to be the preferred structures for each fragment species. The trans isomer is the more stable for each species, with the cis isomer being electronically strained by 10.5 and 5.8 kcal/mol in the neutral and cationic fragments, respectively.

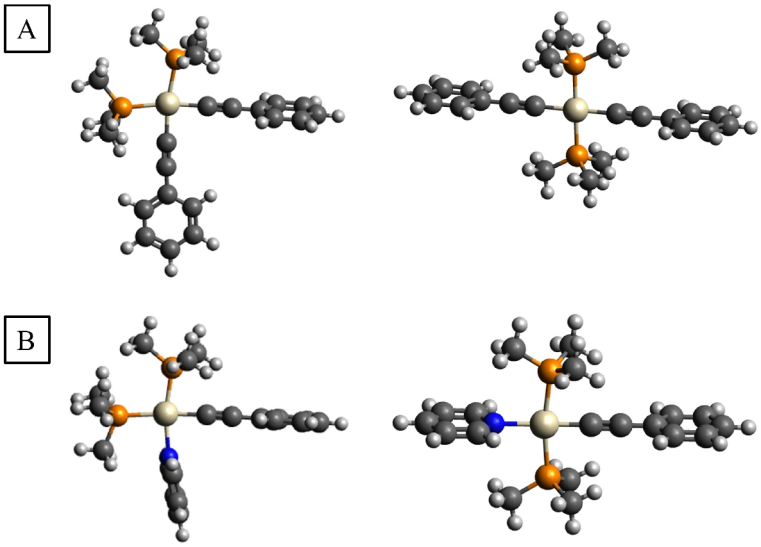

Figure 3. Optimized geometries for cis and trans isomers of (A) neutral and (B) cationic platinum-centered fragments.

Table 2. Relative PBE0/Def2-TZVPP Energies of Optimized Fragment Isomers (kcal/mol).[a,b]

Fragment	$E_{rel\text{-}strain}$(elec)	
	1	**2**
trans	0.0	0.0
cis	10.5	5.8

[a] See Figure 3.

[b] The energy of the most stable isomer is -1656.340 a.u. for **1** and -1596.689 a.u. for **2**.

Mechanical Strain. To investigate the mechanical strain induced by ring formation, we again use the platinum-centered fragments shown in Figure 3. Each macrocycle is divided into four fragments by cutting the central C-C bonds in the four rods and capping with terminal hydrogens. The numbers next to each platinum in Figure 2 correspond to the fragment number in Table 3. The quantity E_{strain}(mech) shown in Table 3 is the energy of a fragment distorted to its geometry in the macrocycle shown in Figure 2, relative to the corresponding cis or trans fragment with all coordinates optimized (Figure 3). The geometries of these fragments are taken from the optimized geometries of the macrocycles and have the positions of the two added terminal hydrogens optimized. Their positions are constrained to be along the line of the C-C bond which was cut to retain some of the strain.

Table 3. Mechanical Strain in Macrocycle Fragments (kcal/mol).

Compd./Fragment	E_{strain}(mech)	Compd./Fragment	E_{strain}(mech)
1		**2**	
t_4		**t_4**	
1	9.17	1	13.21
2	9.90	2	13.55
3	10.20	3	13.18
4	10.46	4	13.53
sum	39.74	sum	53.46
ct_3		**ct_3**	
1	4.58	1	3.02
2	6.12	2	11.54
3	15.53	3	18.64
4	7.05	4	8.14
sum	33.28	sum	41.34
ctct		**ctct**	
1	5.96	1	5.70
2	4.23	2	4.80
3	4.16	3	5.70
4	4.53	4	4.80
sum	18.87	sum	21.00
cttc		**ct:tc**	
1	9.76	1	3.39
2	11.17	2	3.53
3	2.88	3	12.28
4	4.45	4	11.76
sum	28.26	sum	30.96
c_3t		**c_3t**	
1	3.6	1	3.23
2	3.37	2	8.82
3	5.19	3	3.85
4	7.08	4	4.57
sum	19.24	sum	20.46
c_4		**c_4**	
1	4.41	1	3.38
2	2.59	2	3.30
3	2.56	3	3.50
4	4.13	4	3.32
sum	13.69	sum	13.51

Using the relative electronic strain in the optimized cis and trans fragments in Table 2 and the mechanical strain in each fragment at its macrocyclic geometry from Table 3, the total ring strain can be approximated for each macrocycle isomer by summing the mechanical and the electronic strain in all four of its fragments {'total ring strain' = $\Sigma[E_{strain}(\text{mech})] + E_{rel\text{-}strain}(\text{elec})\times(\#\text{ of cis Pt})$ }. Calculating the total ring strain in each macrocycle and subtracting that of the most stable isomer for each species gives the relative total strain $E_{rel\text{-}strain}$(tot) for each macrocycle, which is an approximation

to its relative energy, E_{rel}. The results of these calculations are shown in Table 4, where E_{rel} is the relative energy of a macrocycle from Table 1.

Table 4: Relative Macrocycle Energies Calculated from Electronic and Mechanical Strain in Fragments (kcal/mol).

Compd.	E_{rel}	$E_{rel\text{-}strain}$(tot)	Error
1			
$\mathbf{t_4}$	0.0	0.0	0.0
$\mathbf{ct_3}$	4.2	4.0	-0.2
ctct	0.4	0.1	-0.3
cttc	9.8	9.5	-0.3
$\mathbf{c_3t}$	11.4	10.9	-0.5
$\mathbf{c_4}$	17.2	15.9	-1.3
2			
$\mathbf{t_4}$	37.6	16.8	-20.8
$\mathbf{ct_3}$	24.5	10.5	-14.0
ctct	0.4	-4.1	-4.5
ct:tc	13.8	5.9	-7.9
$\mathbf{c_3t}$	3.0	1.2	-1.8
$\mathbf{c_4}$	0.0	0.0	0.0

The small difference between $E_{rel\text{-}strain}$(tot) and E_{rel} illustrates the additivity of the electronic and mechanical forms of strain in the six neutral macrocycles **1**. The errors are almost all under 0.5 kcal/mol and the trend in relative isomer energies is reproduced.

Unlike the energies of their neutral counterparts, the relative energies of the six isomers of the cationic macrocycle **2** are not reproduced well by summing their relative electronic and mechanical strain. The differences between $E_{rel\text{-}strain}$(tot) and E_{rel} are large and increase with the number of trans fragments in the macrocycle. The trend in relative energies is nevertheless mostly reproduced, except that the **ctct** isomer is predicted to be the most stable. The large discrepancies are probably due to electrostatic interactions among the four fragments in each macrocycle, which are neglected in the calculation of $E_{rel\text{-}strain}$(tot). This interaction could be called electrostatic strain and should be much greater among the charged fragments in **2** than among the neutral fragments in **1**.

Electrostatic Strain. This quantity is less well defined than the two types of strain that have been considered so far, as it depends on the choice of counterions and of solvent. The classical electrostatic interactions between each pair of fragments in each macrocycle in vacuum were calculated for all neutral and cationic species using both Mulliken and NBO charge distributions, represented by point charges on atoms. The electrostatic interaction energies between each fragment in each macrocycle in vacuum are provided in the Supporting Information (Tables S5 through S8) and the relative electrostatic interaction energy for each macrocycle isomer is given in Table 5 as $E_{rel\text{-}strain}$(ES). We use only the NBO charges in the following.

Table 5: Relative Electrostatic Interaction Between Fragments (kcal/mol).

1	$E_{rel\text{-}strain}$(ES)	**2**	$E_{rel\text{-}strain}$(ES)
$\mathbf{t_4}$	0.0	$\mathbf{t_4}$	32.1
$\mathbf{ct_3}$	0.3	$\mathbf{ct_3}$	22.6
ctct	1.0	**ctct**	14.9
cttc	0.8	**ct:tc**	9.4
$\mathbf{c_3t}$	2.0	$\mathbf{c_3t}$	8.3
$\mathbf{c_4}$	3.0	$\mathbf{c_4}$	0.0

As suspected, the interactions are small in isomers of macrocycle **1** and large in the isomers of **2**. Table 6 provides E_{rel} and $E_{rel\text{-}strain}$(tot) from Table 4 as well as $E_{rel\text{-}strain}$(tot/ES) with the electrostatic correction from NBO charge distribution analysis for comparison.

Table 6: Relative Macrocycle Energies Calculated from Electronic, Mechanical, and Electrostatic Strain (kcal/mol).

Compd.	E_{rel}	$E_{rel\text{-}strain}$(tot)	$E_{rel\text{-}strain}$(tot/NBO)	Error	Error (NBO)
1					
$\mathbf{t_4}$	0.0	0.0	0.0	0.0	0.0
$\mathbf{ct_3}$	4.2	4.0	4.3	-0.2	0.1
ctct	0.4	0.1	1.1	-0.3	0.7
cttc	9.8	9.5	10.3	-0.3	0.5
$\mathbf{c_3t}$	11.4	10.9	12.9	-0.5	1.4
$\mathbf{c_4}$	17.2	15.9	18.9	-1.3	1.7
total				2.7	4.4
2					
$\mathbf{t_4}$	37.6	16.8	48.9	-20.8	11.4
$\mathbf{ct_3}$	24.5	10.5	33.1	-14.0	8.6
ctct	0.4	-4.1	10.8	-4.5	10.4
cttc	13.8	5.9	15.3	-7.9	1.5
$\mathbf{c_3t}$	3.0	1.2	9.4	-1.9	6.4
$\mathbf{c_4}$	0.0	0.0	0.0	0.0	0.0
total				49.0	38.3

In the neutral species **1**, the correction for electrostatics does not provide any improvement. The energy trend remains the same but the correction is excessive. In the charged macrocycle **2**, the electrostatic correction improves the accuracy of the predicted strain. The total absolute error is reduced for all isomers of **2** by ~11 kcal/mol and the $\mathbf{2c_4}$ isomer is correctly identified as the lowest energy isomer. The correction is too large for **2ctct**, which is predicted to be less stable than $\mathbf{2c_3t}$ as opposed to being nearly as stable as $\mathbf{2c_4}$. However, it correctly places **2cttc** above **2ctct** in energy.

Cycle Formation. Experimental evidence shows that the most stable isomer of macrocycle of **1**, the all-trans isomer $\mathbf{1t_4}$, is formed while **2** forms no cycle but linear all-trans oligomers instead.[14] Geometry optimizations of linear tetramers (macrocycles opened at a Pt-C or Pt-N bond) of **1** and **2** could not be converged to determine the energy difference between the macrocycle and linear tetramer; however, as a proxy, the sum of the mechanical strains in the four fragments of a

macrocycle from Table 3 can serve as a good approximation in the case of macrocycle **1** and less so for **2** based on their errors. Macrocycle opening for **1** and **2** also involves breaking a Pt-C or Pt-N bond and inserting HI or NO_3^-. This is approximated for the macrocycles using optimized fragments as shown for the trans case in Figure 4. The cis case is similar in the obvious way. The energy changes associated with these reactions are provided in Table 7.

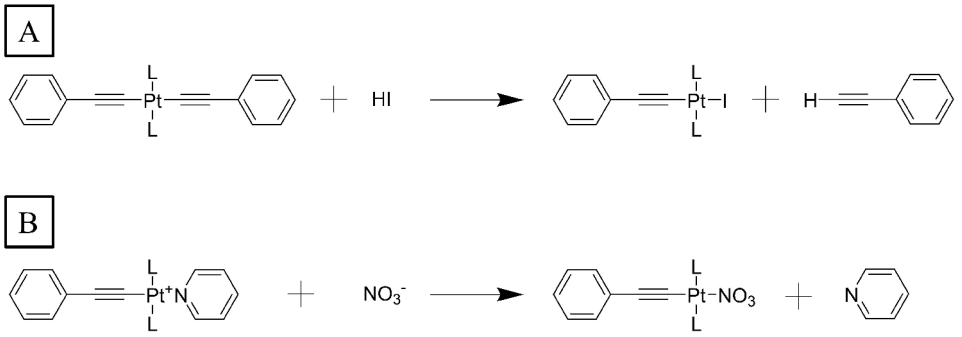

Figure 4. Model cycle-opening reactions for (A) neutral and (B) cationic platinum-centered fragments. Reactions for trans isomers shown.

Table 7. PBE0/Def2-TZVPP Energies of Model Macrocycle Opening Reactions (kcal/mol).

Fragment	ΔE_{rxn}	
	1	**2**
trans	-19.5	-79.1
cis	-20.7	-74.2

The sum of the four fragment mechanical strains for the $\mathbf{1t_4}$ isomer is 39.7 kcal/mol while it is 53.5 kcal/mol for $\mathbf{2t_4}$ (Table 3: sum rows). These are the energies required to distort a linear tetramer (approximated as four electrostatically non-interacting optimized fragments from Figure 3) to the geometry of the all-trans macrocycles. The macrocycle closing reaction of Figure 4 itself then requires an additional 19.5 or 79.1 kcal/mol for **1** and **2**, respectively (Table7: trans row). Macrocycle formation would then be approximately endothermic by 59.2 kcal/mol for $\mathbf{1t_4}$ and endothermic by at least 132.6 kcal/mol for $\mathbf{2t_4}$ by summing the total mechanical strain and macrocycle closing reaction energy for each species. Addition of the electrostatic strain is insignificant for **1** but increases the endothermicity considerably for $\mathbf{2t_4}$. In vacuum, the endothermicities become 73.1 kcal/mol for $\mathbf{1t_4}$ and 288.4 for $\mathbf{2t_4}$. The numbers would be smaller in solution and in the presence of counterions.

Discussion

Why does **1** prefer the mechanically highly strained all-trans isomer $\mathbf{1t_4}$ instead of the all-cis isomer $\mathbf{1c_4}$, like **2** does? This must be a result of a competition between increasing mechanical strain by introducing trans platinum centers and increasing electronic strain by introducing cis centers. Macrocycle formation mechanically strains the cis fragments by 2.6 to 6.0 kcal/mol and the trans fragments by 4.2 to 18.6 kcal/mol, while each cis center induces 10.5 kcal/mol of electronic strain in **1** and 5.8 kcal/mol in **2**. The preference for the trans arrangement of ligands on the Pt atom is not

a surprise. Trans isomers of platinum(II) complexes are generally found to be lower in energy than their cis counterparts and this has been attributed to a difference in unfavorable ligand-ligand electrostatic interactions.[33] The electrostatic interactions within each fragment that we calculate within the point charge approximation (Tables S5 - S8) indeed show that trans fragments in **1** have much lower electrostatic interaction energy than the cis ones. For the cationic macrocycles **2**, the trans and cis fragments have effectively the same internal electrostatic interaction energy and the small preference for the trans macrocycle is likely dominated by steric effects.[34]

We find that the effects of the three types of strain are additive and provide an answer to the question posed above. In **1**, the electronic strain is larger, overruling the smaller mechanical strain, and $\mathbf{1t_4}$ is the preferred isomer. In the cationic macrocycles **2**, the electronic strain due to cis platinum centers is reduced, the mechanical strain overrules electronic, and $\mathbf{2c_4}$ is the most stable isomer. The electrostatic strain plays a negligible role in **1** and favors the $\mathbf{2c_4}$ isomer in **2**.

Mechanical strain is generally larger in cationic fragments than in their neutral counterparts. This is likely due in part to the bipyridyl rods being shorter and therefore requiring more distortion to form the macrocycle ring than the bis(ethynyl)biphenyl rods. The geometries of the **ctct** isomers for both macrocycles **1** and **2** allow the two trans centers to be only slightly curved, resulting in the lowest mechanical strain for trans fragments in any of the isomers. Increasing the number of trans fragments in a macrocycle generally increases the total mechanical strain, with **ctct** isomers being the exception. Although the **1ctct** isomer appears energetically competitive with $\mathbf{1t_4}$, the observed NMR spectra of **1** contain no indication that cis-Pt arrangements are present in the molecule. If the molecule is dynamic on the NMR time-scale, it spends only a minor fraction of time in the **1ctct** form.

An evaluation of the endothermicity of a macrocyclization of the linear tetramer shows that the process is very unfavorable in both instances, particularly for **2**, and this is hardly a surprise. It thus seems unlikely that the linear tetramers, once formed, would ever cyclize, especially the cationic one. The fact that the formation of $\mathbf{1t_4}$ is actually observed suggests that the macrocyclization by self-assembly occurs early in the process, before the linear tetramer is formed, as proposed in the mechanism outlined in the earlier experimental paper.[14] The fact that the even much more endothermic **2** is not formed at all is understandable.

Summary

The favored geometrical structure of the macrocycles **1** and **2** can be understood to result from a competition between three factors, which we refer to as electronic strain, for which trans isomers are favored, mechanical strain, for which cis isomers are favored, and electrostatic strain. Their effects are approximately additive. In the neutral macrocycles **1**, only the electronic and the mechanical strain are important and the former prevails. In the most stable $\mathbf{1t_4}$ isomer, all platinum atoms are trans and the macrocycle is oval-shaped and planar. In the cationic macrocycles **2**, all three types of strain are important and mechanical and electrostatic strain prevail. All platinum atoms are cis, and the macrocycle is rectangular and puckered.

Conflict of Interest Statement. The authors do not have any financial conflicts of interest.

Supporting Information. Large figures showing the structures of all isomers for both compounds, analysis of the effect of the RIJCOSX approximation and the neglect of the dispersion correction, and tables with the calculated electrostatic interaction energy between fragments in all isomers.

Acknowledgement. Work in Boulder was supported by the U.S. National Science Foundation (CHE 1566435). Work in Prague was supported by the Institute of Organic Chemistry and Biochemistry, Academy of Sciences of the Czech Republic (RVO: 61388963). Calculations utilized the RMACC Summit[35] supercomputer, which is supported by the National Science Foundation (awards ACI-1532235 and ACI-1532236), the University of Colorado Boulder, and Colorado State University. The Summit supercomputer is a joint effort of the University of Colorado Boulder and Colorado State University.

References

1. Lehn, J.-M. Toward self-organization and complex matter. *Science* **2002**, *295*, 2400-2403.

2. Fujita, M. Metal-directed self-assembly of two-and three-dimensional synthetic receptors. *Chem. Soc. Rev.* **1998**, *27*, 417-425.

3. Holliday, B. J.; Mirkin, C. A. Strategies for the construction of supramolecular compounds through coordination chemistry. *Angew. Chem., Int. Ed.* **2001**, *40*, 2022-2043.

4. Caulder, D. L.; Raymond, K. N. The rational design of high symmetry coordination clusters. *J. Chem. Soc., Dalton Trans.* **1999**, *8*, 1185-1200.

5. Chakrabarty, R.; Mukherjee, P. S.; Stang, P. Supramolecular coordination: self-assembly of finite two-and three-dimensional ensembles. *J. Chem. Rev.* **2011**, *111*, 6810-6918.

6. Saalfrank, R. W.; Maid, H.; Scheurer, A. Supramolecular coordination chemistry: the synergistic effect of serendipity and rational design. *Angew. Chem., Int. Ed.* **2008**, *47*, 8794-8824.

7. Cotton, F. A.; Lin, C.; Murillo, C. A. Supramolecular arrays based on dimetal building units. *Acc. Chem. Res.* **2011**, *34*, 759-771.

8. Dinolfo, P. H.; Hupp, J. T. Supramolecular coordination chemistry and functional microporous molecular materials. *Chem. Mater.* **2001**, *13*, 3113-3125.

9. Liu, L.; Liu, Z.; Xu, W.; Xu, H.; Zhang, D.; Zhu, D. Syntheses, optical and electrochemical properties of 4, 4 -bis-[2-(3, 4-dibutyl-2-thienylethynyl)] biphenyl and its oligomers. *Tetrahedron* **2005**, *61*, 3813-3817.

10. Anderson, H. L.; Walter, C. J.; Vidal-Ferran, A.; Hay, R. A.; Lowden, P. A.; Sanders, J. K. M. Octatetrayne-linked porphyrins: 'stretched' cyclic dimers and trimers with very spacious cavities. *J. Chem. Soc. Perkin Trans.* **1995**, *18*, 2275-2279.

11. Long, J. R.; Yaghi, O. M. The pervasive chemistry of metal-organic frameworks. *Chem. Soc. Rev.* **2009**, *38*, 1213-1214.

12. Zhou, H-C., Kitagawa, S. Metal-organic frameworks (MOFs). *Chem. Soc. Rev.* **2014**, *43*, 5415-5418.

13. Olive, A. G. L.; Parkan, K.; Givelet, C.; Michl, J. Covalent stabilization: A sturdy molecular square from reversible metal–ion directed self–assembly. *J. Am. Chem. Soc.* **2011**, *133*, 20108-20111.

14. Plutnar, J.; Givelet, C.; Lemouchi, C.; Dytrtová-Jaklová, J.; Teat, S. J.; Michl, J. Mechanical vs. electronic strain: Oval-shaped Alkynyl-Pt(II)-Phosphine macrocycles. *Organometallics* **2019**, *38*, 4633-4644.

15. Adamo, C.; Barone, V. Toward reliable density functional methods without adjustable parameters: The PBE0 model. *J. Chem. Phys.* **1999**, *110*, 6158-6170.

16. Neese, F. The ORCA program system. *Wiley Interdiscip. Rev.: Comput. Mol. Sci.* **2012**, *2*, 73-78.

17. Bühl, M.; Reimann, C.; Pantazis, D. A.; Bedrow, T.; Neese, F. Geometries of third-row transition-metal complexes from density-functional theory. *J. Chem. Theory Comput.* **2008**, *4*, 1449-1459.

18. Grimme, S. Accurate calculation of the heats of formation for large main group compounds with spin-component scaled MP2 methods. *J. Phys. Chem.* A **2005**, *109*, 3067-3077.

19. Andrae, D.; Haeussermann, U.; Dolg, M.; Stoll, H.; Preuss, H. Energy-adjusted *ab initio* pseudopotentials for the second and third row transition elements. *Theor. Chim. Acta,* **1990**, *77*, 123-141.

20. Weigend, F. Accurate Coulomb-fitting basis sets for H to Rn. *Phys. Chem. Chem. Phys.* **2006**, *8*, 1057-1065.

21. Weigend, F.; Ahlrichs, R. Balanced basis sets of split valence, triple zeta valence and quadruple zeta valence quality for H to Rn: Design and assessment of accuracy. *Phys. Chem. Chem. Phys.* **2005**, *7*, 3297-3305.

22. Dolg, M.; Wedig, U.; Stoll, H.; Preuss, H. Energy adjusted *ab initio* pseudopotentials for the first row transition elements. *J. Chem. Phys.* **1987**, *86*, 866-872.

23. Dolg, M. In *Modern Methods and Algorithms of Quantum Chemistry, Proceedings,* 2nd ed.; Grotendorst, J., Ed.; John von Neumann Institute for Computing: Jülich, Germany, 2000; NIC Series Vol. 3, pp 507-540.

24. van Lenthe, E.; Snijders, J. G.; Baerends, E. J. The zero order regular approximation for relativistic effects: The effect of spin–orbit coupling in closed shell molecules. *J. Chem. Phys.* **1996**, *105*, 6505-6516.

25. Izsák, R.; Neese, F. An overlap fitted chain of spheres exchange method. *J. Chem. Phys.* **2011**, *135*, 144105.

26. Neese, F.; Wennmohs, F.; Hansen, A.; Becker, U. Efficient, approximate and parallel Hartree–Fock and hybrid DFT calculations. A 'chain-of-spheres' algorithm for the Hartree–Fock exchange. *Chem. Phys.* **2009**, *356*, 98-109.

27. Weigend, F. Accurate Coulomb-fitting basis sets for H to Rn. *Phys. Chem. Chem. Phys.* **2006**, *8*, 1057-1065.

28. Grimme, S.; Anthony, J.; Ehrlich, S.; Krieg, H. A consistent and accurate *ab initio* parametrization of density functional dispersion correction (DFT-D) for the 94 elements H-Pu. *J.*

Chem. Phys. **2010**, *132*, 154104.

29. Mulliken, R. S. Electronic population analysis on LCAO–MO molecular wave functions. I. *J. Chem. Phys.* **1955**, *23*, 1833.

30. Weinhold, F. Natural bond orbital analysis: A critical overview of relationships to alternative bonding perspectives. *J. Comp. Chem.* **2012**, *33*, 2363-2379.

31. Reed, A. E.; Weinstock, R. B.; Weinhold, F. Natural population analysis. *J. Chem. Phys.* **1985**, *83*, 735-746.

32. NBO 6.0. E. D. Glendening, J, K. Badenhoop, A. E. Reed, J. E. Carpenter, J. A. Bohmann, C. M. Morales, C. R. Landis, and F. Weinhold, Theoretical Chemistry Institute, University of Wisconsin, Madison (2013).

33. Anastasi, A. E.; Deeth R. J. Capturing the trans influence in low-spin d^8 square-planar platinum(II) systems using molecular mechanics. *J. Chem. Theory Comput.* **2009**, *5*, 2339-2352.

34. Packett, D. L.; Jensen, C. M.; Cowan, R. L.; Strouse, C. E.; Trogler, W. C. Syntheses, structures, and mechanism of formation of trans-chlorohydrobis(trimethylphosphine)platinum(II) and trans-dihydrobis(trimethylphosphine)platinum(II). Energetics of cis-trans isomerization. *Inorg. Chem.* **1985**, *24*, 3578-3583.

35. Anderson, J.; Burns, P. J.; Milroy, D.; Ruprecht, P.; Hauser, T.; Siegel, H. J. *Deploying RMACC Summit: An HPC Resource for the Rocky Mountain Region*, in Proceedings of PEARC17, New Orleans, LA, USA, July 09-13, **2017**, 7 pages. DOI: 10.1145/3093338.3093379

TOC Graphic